Histidine 190-D1 and Glutamate 189-D1 Provide Structural Stabilization in Photosystem II†

Idelisa Pujols-Ayala‡ and Bridgette A. Barry*

Department of Biochemistry, Molecular Biology, and Biophysics, University of Minnesota, St. Paul, Minnesota 55108-1022

Received May 22, 2002; Revised Manuscript Received July 22, 2002

ABSTRACT: In photosynthesis, photosystem II (PSII) conducts the light-driven oxidation of water to oxygen. Tyrosine Z is Tyr 161 of the D1 polypeptide; Z acts as an intermediary electron carrier in water oxidation. In this report, EPR spectroscopy was used to study the effect of His 190 and Glu 189 on Z• yield and reduction kinetics. Neither mutation has a significant impact on the EPR line shape of Z•. At room temperature and pH 7.5, the E189Q-D1 mutation has a single turnover Z• yield that is 84% compared to wild-type. The H190Q-D1 mutation decreases the Z• yield at room temperature by a factor of 2.6 but has a more modest effect (factor of 1.6) at −10 °C. The temperature dependence is shown to be primarily reversible. Neither mutation has a dramatic effect on Z• decay kinetics. The Z• minus Z FT-IR spectrum, recorded at pH 7.5 on H190Q, reveals perturbations, including an increased spectral contribution from a PSII chlorophyll. The Z• minus Z FT-IR spectrum, recorded at pH 7.5 on E189Q, shows perturbations, including a decreased contribution from the carboxylate side chain of a glutamate or aspartate. Temperature-dependent changes in H190Q-D1 and E189Q-D1 Z• yield are attributed to a reversible conformational change, which alters the electron-transfer rate from Z to P_{680}^+. On the basis of these results, we conclude that H190 and E189 play a role in the structural stabilization of PSII. We postulate that some or all of the phenotypic changes observed in H190Q and E189Q mutants may be caused by structural alterations in PSII.

Photosystem II (PSII)[1] is a multisubunit enzyme that is found in higher plants, green algae, and cyanobacteria. PSII conducts the oxidation of water to molecular oxygen and the reduction of plastoquinone in oxygenic photosynthesis. These processes are driven by light and involve both cofactors and redox-active amino acids. Upon light absorption by the primary electron donor, P_{680}, an electron is transferred to Q_A, a single electron acceptor, and then to Q_B, which is a two-electron acceptor. P_{680}^+ is reduced by a redox-active tyrosine residue, Z, forming a neutral, unprotonated radical, Z•. Z• is in turn reduced by the manganese cluster in the microsecond to millisecond time scale. The manganese cluster is the catalytic site for water oxidation, and four sequential charge separations are required to release molecular oxygen. The kinetics of Z• reduction can be altered by removal of the manganese cluster, in which case Z• will be reduced by an exogenous electron donor or by recombination with the quinone acceptors. PSII contains another redox-active tyrosine residue, D, which has a long lifetime in the oxidized form (reviewed in refs *1* and *2*). A 3.8 Å structural model of cyanobacterial PSII has been presented recently (*3*, *4*).

EPR spectroscopy, isotopic labeling, and site-directed mutagenesis identified tyrosine Z as residue 161 of the D1 polypeptide (*5*−*8*) and tyrosine D as residue 160 of the D2 polypeptide (*9*−*11*). While the two redox-active tyrosine residues are in symmetric positions in the reaction center (*12*−*15*), these two residues differ in the rate of decay and in midpoint potential (*16*−*18*). These functional differences may be imposed by differences in the interaction of Z and D with their protein environments. Because D• and Z• are neutral radicals, proton transfer may accompany the oxidation and reduction reactions. Therefore, protein dielectric and polarity, hydrogen-bonding interactions, and differences in the pK_a of the proton-accepting group can alter the midpoint potential and kinetics of these redox-active groups.

Previous structural models of PSII (*13*, *14*), based on the bacterial reaction center structure, suggested that His 190 and Glu 189 of the D1 polypeptide might be in close proximity to tyrosine Z. All mutations at His 190 and many mutations at Glu 189 inactivate oxygen evolution (*19*−*25*). It has been suggested that His 190 may influence the redox properties of Z or may provide ligation to manganese (for example, see ref *23*). It has also been suggested that Glu 189 may be involved in a hydrogen-bonding network surrounding Z and/or may act as an auxiliary proton acceptor in photosystem II (*23*−*25*).

† Supported by NIH Grant GM43273 (B.A.B.) and NIH Predoctoral Fellowship GM19541 (I.P.-A.).

* Author to whom correspondence should be addressed. Telephone: 612-624-6732. Fax: 612-625-5780. E-mail: barry@cbs.umn.edu.

‡ Present address: Department of Pharmacology and Therapeutics, University of Florida, Gainesville, FL 32610.

[1] Abbreviations: chl, chlorophyll; D, tyrosine 160 of the D2 polypeptide of PSII; DCBQ, 2,6-dichloro-*p*-benzoquinone; DCMU, 3-(3,4-dichlorophenyl)-1,1-dimethylurea; EPR, electron paramagnetic resonance spectroscopy; FT-IR, Fourier transform infrared spectroscopy; HEPES, *N*-(2-hydroxyethyl)piperazine-*N*′-2-ethanesulfonic acid; MES, 2-(*N*-morpholino)ethanesulfonic acid; PBQ, *p*-benzoquinone; PSI, photosystem I; PSII, photosystem II; TES, *N*-[tris(hydroxymethyl)-methyl]-2-aminoethanesulfonic acid; Z, tyrosine 161 of the D1 polypeptide of PSII.

10.1021/bi026172l CCC: $22.00
Published on Web 08/24/2002

There are several possibilities for the role of His 190 in tyrosine Z redox reactions. One possibility is that His 190 interacts with tyrosine Z or Z• through a hydrogen-bonding interaction and that removal of His 190 changes the midpoint potential of Z/Z•. However, magnetic resonance studies suggest that hydrogen bonding to Z• is disordered (*26*−*29*), and the identity of the hydrogen-bonding partner for tyrosine Z is still unclear (*19*−*22*, *30*).

A second possibility is that His 190 is involved in proton-transfer reactions accompanying the oxidation and reduction of tyrosine Z. Several studies have probed the pH and ^2H_2O dependence of Z oxidation/Z• reduction in PSII preparations in which the reduction rate has been slowed by removal or by the absence of manganese (*21*, *29*, *31*−*33*). For example, a study of the H190F and H190Y mutations, produced in *Chlamydomonas reinhardtii*, concluded that His 190 is involved in Z•-based proton-transfer reactions (*21*). Chemical complementation studies of cyanobacterial mutants have also been interpreted in that manner (*22*, *30*).

Other studies have concluded that His 190 is not the direct proton acceptor for Z (*19*, *20*), because little change was observed in the EPR and FT-IR spectra of Z• in the H190Q-D1 mutant. This was in contrast to results obtained on tyrosine D using similar approaches; His 189 in the D2 polypeptide is known to be the proton acceptor and hydrogen partner of tyrosine D (see, for example, ref *34* and references therein). Recently, a structural model of PSII, derived from X-ray diffraction, suggests that, actually, H190 and tyrosine Z are not in close proximity in the PSII reaction center (*35*). However, more highly resolved structural information is needed to address this point definitively.

A third possibility is that His 190 plays a role in structural stabilization of the PSII reaction center. The experiments reported here were designed to provide more information concerning the roles of His 190 and Glu 189 in PSII. At low temperature, we find that the yield of Z• is within a factor of 2 in wild-type, H190Q-D1, and E189Q-D1 PSII. Moreover, the yield in the mutants is temperature-dependent and shows a decrease at higher temperatures. There is no significant effect of either mutation on Z• decay kinetics at any temperature. In combination with difference FT-IR spectroscopy, these studies suggest that His 190 and Glu 189 play a role in stabilization of the PSII donor side and that neither His 190 nor Glu 189 functions as the immediate proton acceptor for tyrosine Z.

MATERIALS AND METHODS

Cyanobacterial Growth and Site-Directed Mutagenesis. For experiments on wild-type, E189Q-D1, and H190Q-D1, the appropriate strain of *Synechocystis* sp. PCC 6803 was grown photoheterotrophically (*1*) in BG-11 media containing 5 mM TES−NaOH, pH 8.0, and 5 mM glucose (*36*, *37*). The cultures grew for approximately 6−7 days under constant illumination at 30 °C until an OD_{730} of 1−1.5 was reached. The cells were harvested by centrifugation and frozen at −80 °C in a buffer containing 20 mM MES−NaOH, pH 6.0, 20 mM $MgCl_2$, 20 mM $CaCl_2$, and 25% glycerol.

The construction of the H190Q-D1 mutant strain has been described previously (*20*). The E189Q-D1 mutation was constructed by standard techniques (*37*). Briefly, a *Synechocystis* strain, lacking all three copies of the D1 gene, was transformed with a plasmid containing the psbA-2 gene and a kanamycin resistance cassette (ATG Laboratories, Eden Prairie, MN). The psbA-2 gene was modified to code for the E189Q-D1 mutation (ATG Laboratories). Transformants were selected by plating cells on kanamycin. To verify the presence of the mutation, genomic DNA was isolated. PCR amplification was performed using oligonucleotides designed (Microchemical Facilities, University of Minnesota, Minneapolis, MN) to amplify the psbA-2 gene. Sequencing was performed at the DNA Sequencing and Synthesis Facility at Iowa State University (Ames, IA). The presence of the H190Q-D1 and E189Q-D1 mutations was verified by sequencing the genes from both the 5′ and the 3′ ends. In the H190Q-D1 and E189Q-D1 strains, either H190Q-D1 or E189Q-D1, respectively, was the only mutation in the D1 coding region. Sequencing of the H190Q-D1 mutant, which is photoheterotrophic and likely to revert, was performed both before and after the experiments reported here.

Photosystem II Purification. PSII was isolated from wild-type, H190Q-D1, and E189Q-D1 cultures using methods previously described (*1*, *38*). Briefly, thylakoid membranes were prepared from the harvested cells. Two anion-exchange columns were performed to purify PSII. The first was a low-pressure Fast Flow Q-Sepharose column (Pharmacia-Amersham Biosciences, Piscataway, NJ) at pH 6.0. Fractions were pooled, precipitated, and resuspended, as previously described (*1*, *38*). The resuspended material was then loaded onto a HR 5/5 Mono Q FPLC column (Pharmacia-Amersham Biosciences) in order to remove remaining PSI contamination (*1*, *38*). Photosystem I (PSI) was also isolated from wild-type cultures (*39*).

Chlorophyll and Oxygen Evolution Assays. Chlorophyll concentrations were determined in 100% methanol (*40*). Oxygen rates were measured as described (*1*). Oxygen rates were as follows: wild-type, 2000 μmol of O_2 (mg of chl)$^{-1}$ h^{-1}; H190Q-D1, <30 μmol of O_2 (mg of chl)$^{-1}$ h^{-1}; E189Q-D1, 1000 μmol of O_2 (mg of chl)$^{-1}$ h^{-1}.

Manganese Depletion. Wild-type, E189Q-D1, and H190Q-D1 PSII were treated with hydroxylamine, which was then removed by a column chromatography step and overnight dialysis (*20*). This procedure leaves PSII particles that have been shown to contain, on average, one manganese atom per reaction center and are inactive in water oxidation (*41*). As assessed by the steady-state yield of Z•, H190Q-D1 PSII lacks an active manganese cluster (*20*). However, the H190Q-D1 preparation was treated with hydroxylamine to facilitate comparison to wild-type PSII, which must be manganese depleted to slow the reduction of Z•.

Fluorescence Spectroscopy. Fluorescence measurements were performed on a Photon Systems Instruments (Czech Republic) dual-modulation kinetic fluorometer. A single saturating flash from a flash lamp was provided to the sample, which consisted of either intact cells or purified PSII. The fluorometer was equipped with the standard Photon Systems filter package. A 700 nm band-pass (25 nm) filter and 695 nm high-pass filter were mounted in front of the detector. The illumination from the xenon lamp was blue and heat filtered. The measurements were performed on aqueous samples. The yield and decay of fluorescence were measured after a single flash at room temperature. The first data point was acquired 200 μs after the flash, to allow the decay of a flash lamp-derived artifact.

For measurements on intact cells, 10 μg of chl in 1.2 mL of buffer containing 50 mM MES−NaOH, pH 6.5, 25 mM $CaCl_2$, and 10 mM NaCl was employed. Data acquisition was initiated after the sample was incubated in the dark for 10 min in the presence of 40 μM DCMU. DCMU blocks electron transfer to Q_B (*42*). The final ethanol concentration was 0.8%. For measurements on manganese-depleted PSII particles, 10 μg of chl in 1.2 mL of buffer containing 5 mM HEPES−NaOH, pH 7.5, 3 mM potassium ferricyanide, and 3 mM potassium ferrocyanide was employed. In some PSII experiments, 100 μM DCMU was employed. In those cases, the final ethanol concentration was 2%. For both types of samples, spectral conditions were as follows: flash duration, 10 μs; measuring flash voltage, 25%; actinic flash voltage, 100%. Data are the average of 6−12 traces acquired on two to three samples. There was 5 min between the flashes.

EPR Spectroscopy. Spectra were recorded on a Bruker EMX 6/1 spectrometer (Billerica, MA). PSII measurements were performed on partially dehydrated and on aqueous manganese-depleted samples. For dehydrated samples, a Wilmad (Buena, NJ) variable temperature dewar was employed, and field-swept spectra were collected at either −10, 4, or 21 °C. The temperature was varied by controlling the nitrogen flow rate through an ethanol−dry ice bath (*43*). Samples had a chlorophyll concentration of 1 mg/mL, and the buffer was 5 mM HEPES−NaOH, pH 7.5, 3 mM potassium ferricyanide, and 3 mM potassium ferrocyanide. An aliquot containing 120−140 μg of chl was partially dehydrated on Mylar strips using a stream of nitrogen. Spectral conditions were as follows: microwave frequency, 9.21 GHz; microwave power, 0.8 or 2 mW; modulation amplitude, 3−3.5 G; scan time, 4 min; and time constant, 1.3 s.

Measurements on liquid samples were performed in a flat cell at room temperature. Samples had a total volume of 250 μL and contained 150 μg of chl, 5 mM HEPES−NaOH, pH 7.5, 3 mM potassium ferricyanide, and 3 mM potassium ferrocyanide. Data acquisition conditions for field-swept spectra were as follows: microwave frequency, 9.74 GHz; microwave power, 12.7 mW; modulation amplitude, 3−3.5 G; scan time, 4 min; and time constant, 1.3 s.

The decay of the tyrosyl radical Z$^\bullet$ in wild-type, H190Q-D1, and E189Q-D1 was monitored at a constant magnetic field. The illumination source was the second harmonic of a Continuum (Santa Clara, CA) Nd:YAG laser, which produces 7 ns pulses at 532 nm (*43*). The sample was flashed every 5 s, and the EPR transient was recorded. For samples that were partially dehydrated, the following spectral parameters were employed: microwave frequency, 9.21 GHz; microwave power, 12.7 mW; modulation amplitude, 5 G; scan time, 1.3 s; and time constant, 10.2 ms. The data shown are an average of 97−327 traces. For liquid samples, the spectral parameters were as follows: microwave frequency, 9.74 GHz; microwave power, 12.7 mW; modulation amplitude, 5 G; scan time, 1.3 s; and time constant, 10.2 ms. The number of data points was 512, and data shown are an average of 289−300 traces. The data were fit and analyzed with IGOR Pro software (Lake Oswego, OR).

FT-IR Spectroscopy. Spectra were recorded on a Nicolet (Madison, WI) Magna 550 II spectrometer equipped with a MCT-A detector. Data were acquired using 4 min or 1.3 s of illumination on partially dehydrated samples at −10 °C. This is necessary to reduce the contribution of water to the spectrum. A Z$^\bullet$ minus Z difference FTIR spectrum was constructed as previously described (*43*−*45*). Manganese-depleted PSII (30 μL) from wild-type, H190Q-D1, and E189Q-D1 was employed. Samples had a chl concentration of 1 mg/mL and were in a buffer containing 5 mM HEPES−NaOH, pH 7.5. PSII was partially dehydrated after the addition of 3 mM potassium ferricyanide and 3 mM potassium ferrocyanide. The PSII sample was sandwiched between a Ge window and a CaF_2 window.

When the samples were illuminated for 4 min, the spectral conditions were as follows: resolution, 4 cm^{-1}; number of scans, 425; apodization function, Happ Genzel; levels of zero filling, one; and mirror velocity, 2.5 cm/s. The spectra were normalized using the amide II absorbance (normalized final value: 0.35 absorbance unit). For 4 min data, spectra are an average of 92 (wild-type), 53 (H190Q-D1), and 46 (E189Q-D1).

A P_{700}^+ minus P_{700} difference FTIR spectrum (*39*, *46*) was also obtained from PSI samples, which were isolated from wild-type cyanobacterial cultures. Spectra were recorded on a Nicolet Magna 550 II spectrometer equipped with a MCT-A detector. A 30 μL aliquot of 4−5 mg of chl/mL of sample was partially dehydrated in the presence of 11 mM potassium ferricyanide and 11 mM potassium ferrocyanide. Spectral conditions were as follows: resolution, 4 cm^{-1}; number of scans, 425; apodization function, Happ Genzel; levels of zero filling, two; and mirror velocity, 2.5 cm/s. The spectra were normalized to an amide II absorbance of 0.35. Data shown are an average of 40 spectra.

RESULTS

Fluorescence Measurements. Chl fluorescence was used as an indirect measure of the production and decay of Q_A^- in PSII (*42*). Figure 1A, solid line, presents fluorescence data acquired from intact, wild-type cells in the presence of DCMU. In cells from E189Q-D1 cultures (Figure 1A, dashed line), the yield and decay of chl fluorescence are similar to that of wild-type, as previously reported (*23*). However, in H190Q-D1 cells (Figure 1A, dotted line) there was no significant production and decay of chl fluorescence. The H190Q-D1 result agrees with previous reports of low fluorescence yield in His 190 mutants (*23*, *47*). These results have been interpreted to show a defect in the reduction of P_{680}^+ in the H190Q-D1 mutant.

Z$^\bullet$ has a short half-time in oxygen-evolving PSII (*48*). To increase the decay time of Z$^\bullet$ in wild-type and E189Q-D1, PSII can be depleted of manganese (*16*) by treatment with hydroxylamine (*20*). H190Q-D1, which lacks manganese, was also treated with hydroxylamine, so that all samples would be comparable. The production and decay of chl fluorescence were monitored in manganese-depleted PSII particles from the wild-type and the H190Q-D1 mutant (Figure 1B). These aqueous PSII samples contained 3 mM potassium ferricyanide as an electron acceptor and 3 mM potassium ferrocyanide as an electron donor. Wild-type PSII (Figure 1B, solid line) showed the production and decay of chl fluorescence, consistent with Q_A^- production and decay. As expected, the decay was on a faster time scale when compared to intact wild-type cells, which contain a functional water oxidizing complex (Figure 1A, solid line). In wild-

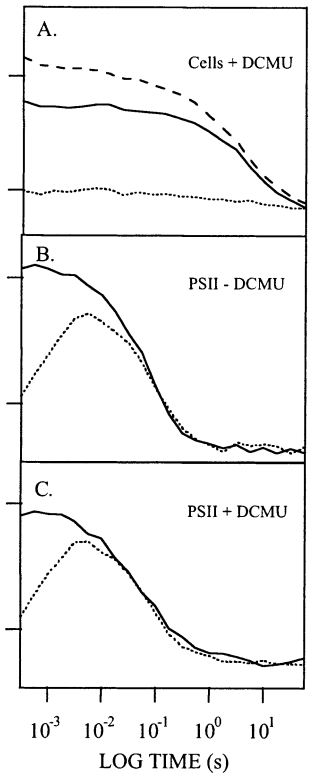

FIGURE 1: The production and decay of chl fluorescence in cells (A) from wild-type (solid line), H190Q-D1 (dotted line), and E189Q-D1 (dashed line) cultures. Panels B and C show the production and decay of chl fluorescence in PSII particles isolated from wild-type (solid line) or the H190Q-D1 mutant (dotted line). Samples in (A) and (C) contained DCMU. All the data were obtained on hydrated samples at room temperature. In each trace, the signal level before the flash corresponds to zero on the *y*-axis. In (A), the tick marks represent 50 mV; in (B) and (C), the tick marks represent 15 mV. Spectral conditions are given in Materials and Methods.

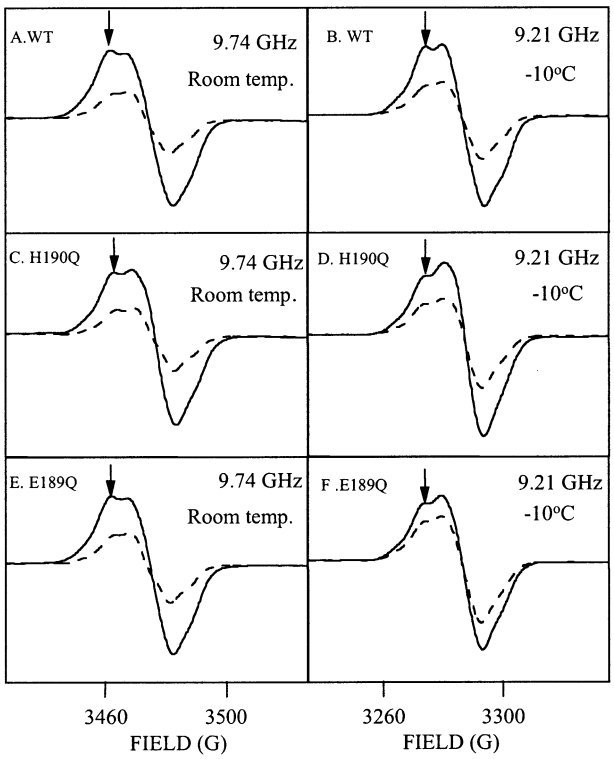

FIGURE 2: Field-swept EPR spectra obtained from wild-type (A and B), H190Q-D1 (C and D), and E189Q-D1 (E and F) manganese-depleted PSII particles. Spectra were collected under two different conditions. Panels A, C, and E show spectra obtained at room temperature on liquid samples. Panels B, D, and F display spectra obtained on partially dehydrated samples at −10 °C. In each panel, the solid line illustrates the spectra obtained under 4 min of continuous illumination, and the dashed line represents spectra acquired after 8 min of dark adaptation. The arrow represents the field position employed for transient EPR measurements (Figures 3 and 4). Spectral conditions are given in Materials and Methods.

type PSII, the overall half-time of fluorescence decay was approximately 50 ms (Figure 1B, solid line).

In H190Q-D1 PSII, a rapid rise in the fluorescence yield after the actinic flash was observed (Figure 1B, dotted line). This increase in chl fluorescence was approximately 31% of the fluorescence yield in wild-type at the first data point (Figure 1B, solid line). Based on EPR measurements (see below), this rapid rise in fluorescence in H190Q-D1 is attributed to PSII centers in which Z reduces P_{680}^{+}. The H190Q-D1 mutant also exhibits a slow accumulation of chl fluorescence after the actinic flash (Figure 1B, dotted line). The increase in chl fluorescence appeared complete in 5 ms and may be due to the slow reduction of an alternate donor, which is a quencher of fluorescence, by potassium ferrocyanide. This slow rise time for chl fluorescence is in qualitative agreement with previous studies of a H190Y mutant in the presence of an exogenous donor (*47*).

The kinetics of fluorescence decay in the H190Q-D1 mutant are expected to be complex due to the superposition of several rates, possibly corresponding to any further increase in fluorescence yield, to recombination events, and to oxidation of Q_A^- by ferricyanide. The overall half-time for these processes was 90 ms (Figure 1B, dotted line).

As expected on the basis of previous work with this PSII preparation (*42*), there was no significant rate change observed in the presence of DCMU (Figure 1C). However, H190Q-D1 cells and H190Q-D1 PSII particles show strikingly different behavior in the fluorescence measurements (compare Figure 1A, dotted line, and Figure 1B, dotted line). This result suggests the presence of a fluorescence quencher in H190Q-D1 cells, which is removed by PSII purification.

Field-Swept EPR Measurements under Continuous Illumination. EPR spectra were recorded under continuous illumination from manganese-depleted cyanobacterial PSII. Panels A, C, and E of Figure 2 show EPR spectra acquired from wild-type, H190Q-D1, and E189Q-D1 PSII, respectively, in liquid samples at room temperature. Under 4 min of continuous illumination (solid lines), both Z• and D• were generated in all three samples. After 8 min of dark adaptation (dashed lines), Z• decayed, and only contributions from D• were observed. D• has a decay time in the minutes to hours time regime (*1*). Note that the EPR spectra acquired from wild-type and mutant PSII have similar, but not identical, line shapes (Figure 2A,C,E). Spin quantitation shows that the Z• yield under illumination is within 30%, when mutants and wild-type samples are compared.

To record the EPR line shape at lower temperatures, measurements were also performed on manganese-depleted PSII samples, which were partially dehydrated on Mylar strips. Spectra were acquired at −10 °C, a temperature at which Z• can be produced in high yield in manganese-

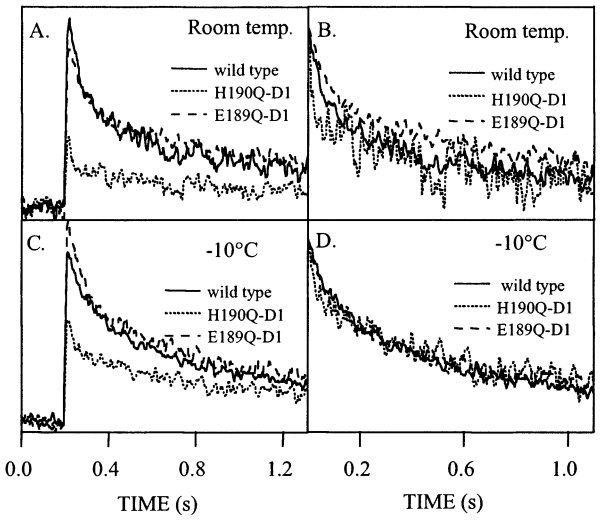

FIGURE 3: Transient EPR measurements of tyrosyl radical Z· decay in wild-type (solid line), H190Q-D1 (dotted line), and E189Q-D1 (dashed line) manganese-depleted PSII. (A) and (B) were acquired from liquid samples at room temperature; (C) and (D) were acquired from partially dehydrated samples at −10 °C. Data in (B) are repeated from (A) and arbitrarily normalized to the same value at the first data point. Data in (D) are repeated from (C) and arbitrarily normalized to the same value at the first data point. Spectral conditions are given in Materials and Methods.

depleted PSII (*49*−*52*). In panels B, D, and F of Figure 2, spectra were recorded from wild-type, H190Q-D1, and E189Q-D1 PSII, respectively, under partially dehydrated conditions. Again, the EPR spectra of mutants and wild-type PSII were observed to be similar, but not identical, to each other. Spin quantitation shows that the yield of Z· was within 30% in all three samples. The small line shape change, when the H190Q-D1 mutant is compared to wild-type, could be consistent with the increased photoaccumulation of a Chl_Z^+ radical, which has a narrow EPR line shape (*53*). All −10 °C spectral line shapes (Figure 2B,D,F) are similar to the room temperature line shapes (Figure 2A,C,E).

Single Turnover EPR Measurements. The yield of Z· on a single turnover was monitored by recording the EPR transient at a constant field position (see arrows on Figure 2). EPR spectroscopy at this field position is specific for the decay of tyrosyl radicals Z· and D· (for a recent example, see ref *51*). There is no significant contribution at this field position from narrow radicals, such as Chl_Z^+, produced in a minor amount under illumination. Samples were flashed with a repetition rate of 0.2 Hz. This repetition rate precludes contributions from tyrosyl radical D·, because this species is dark stable and decays on the order of minutes to hours (Figure 2).

Figure 3A illustrates the decay of Z· in aqueous samples at room temperature. Manganese-depleted PSII particles were isolated from wild-type (solid line), H190Q-D1 (dotted line), and E189Q-D1 (dashed line). In wild-type, Z· was produced with a single flash (Figure 3A, solid line) and decayed with an overall half-time of 140 ms. This half-time agrees with previous EPR measurements on cyanobacterial, wild-type PSII (*54*). The decay of Z· in wild-type was fit with a biexponential function. The derived rate constants for the fast and slow phase were 17.2 ± 6.6 s^{-1} (∼40%) and a 2.5 ± 0.6 s^{-1} (∼40%), respectively. The remaining phase (20%) was nondecaying.

In E189Q-D1 (Figure 3A, dashed line), Z· was produced in 84% yield compared to wild-type. The decay (Figure 3B, dashed line) was fit with a biexponential function with rate constants of 14.6 ± 2.2 s^{-1} (∼40%) and 1.2 ± 0.2 s^{-1} (∼40%) for the fast and the slow phases, respectively. The remaining phase was nondecaying, and the half-time of Z· decay in this mutant was 220 ms. Overall, the kinetics of decay in E189Q-D1 were similar to wild-type.

In the H190Q-D1 mutant (dotted line), the yield of Z· on a single flash was low (≤38%) when compared to wild-type. Although the yield is low, the rate of Z· reduction in the H190Q-D1 mutant was qualitatively similar to the rate observed in wild-type (see normalized traces, Figure 3B). Quantitative fits to the data were not attempted, however, because of the small signal amplitude. These conclusions agree with the results of previous EPR measurements on a H190 mutant (*19*).

The H190Q-D1 transient data can be reconciled with the field-swept EPR data (Figure 2), which showed a Z· yield under continuous illumination that was similar to that of wild-type. With a single turnover, the yield of Z· is small, but under continuous illumination, the radical is photoaccumulated in the mutant. The EPR kinetic data are also consistent with room temperature fluorescence data on H190Q-D1 (Figure 1B, dotted line), which showed a rise in fluorescence in 31% of the PSII centers at the first data point after the flash.

Figure 3C presents the decay of Z· in partially dehydrated, manganese-depleted samples at −10 °C. PSII particles were isolated from wild-type (solid line), H190Q-D1 (dotted line), and E189Q-D1 (dashed line). Surprisingly, at this temperature, Z· was produced with increased yield in the H190Q-D1 mutants, relative to wild-type. There was also an increase in the relative Z· yield in E189Q-D1 PSII. The amount of Z· generated in H190Q-D1 and in E189Q-D1 on a single turnover was 62% and 122%, respectively, of the wild-type yield (Figure 3C). The overall decay half-times were similar, with a value of 250 ms for wild-type, 280 ms for the H190Q-D1 mutant, and 190 ms for the E189Q-D1 mutant (see normalized traces, Figure 3D). All kinetic traces were fit with biexponential functions. The slow phase was indistinguishable in wild-type, H190Q-D1, and E189Q-D1; the rate constants were 2.0 ± 0.9 s^{-1} for wild-type (∼60%), 2.0 ± 0.2 s^{-1} (∼50%) for H190Q-D1, and 1.9 ± 0.2 s^{-1} (∼50%) for E189Q-D1. For the fast phase, H190Q-D1 exhibited the largest rate constant. The rate constants were 18.3 ± 7.1 s^{-1} (∼20%) for wild-type, 55.4 ± 5.7 s^{-1} (∼30%) for H190Q-D1, and 17.0 ± 3.1 (∼30%) for E189Q-D1.

In summary, these single flash EPR data show that the yield of Z· is low in H190Q-D1 at room temperature. However, when the temperature is changed from room temperature to −10 °C, the H190Q-D1 Z· yield *increases*. An increase in relative Z· yield also occurs in the E189Q-D1 mutant. Under these conditions, the Z· decay kinetics are similar in the mutants and wild-type. The only possibly significant change, compared to wild-type, is a 2−3-fold *increase* in the fast phase of Z· reduction in H190Q-D1 at −10 °C. This change, even if significant, cannot explain the increase in Z· yield at −10 °C. We conclude that the changes in Z· yield, observed in the H190Q-D1 and E189Q-D1 mutants, are due to changes in the rate of electron transfer from Z to P_{680}^+. This change could be due to a direct effect

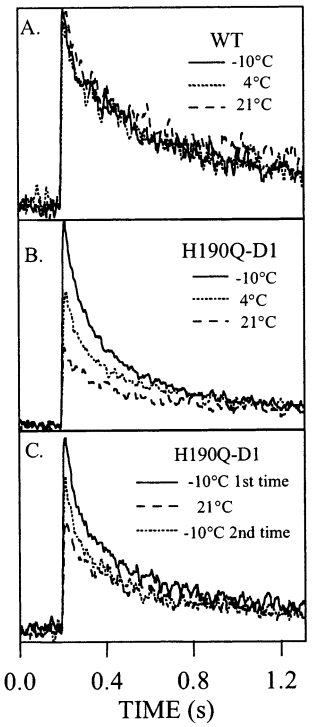

FIGURE 4: Temperature effect on the decay of tyrosyl radical Z· as assessed by transient EPR measurements. Transients were recorded on partially dehydrated manganese-depleted PSII samples. Panels A and B show traces acquired for wild-type and H190Q-D1, respectively, at −10 °C (solid line), 4 °C (dotted line), and 21 °C (dashed line). Panel C shows traces recorded on a partially dehydrated H190Q-D1 sample at −10 °C (solid line), then at 21 °C (dashed line), and finally after reequilibration at −10 °C (dotted line). Spectral conditions are given in Materials and Methods.

on this electron-transfer reaction. For example, a change in the distance between Z and P_{680} may occur. Alternatively, these changes could be due to an indirect effect. Such an indirect effect could occur if the mutations slow a competing rate of electron transfer from an alternate donor to P_{680}^+ at −10 °C.

Temperature Effects on the Single Turnover EPR Measurements. The increase in relative Z· yield observed in Figure 3B could be due to a temperature effect or to the partial dehydration of H190Q-D1 and E189Q-D1 samples. To study the effect of temperature, partially dehydrated, manganese-depleted PSII samples from wild-type and H190Q-D1 were employed. Figure 4A shows EPR transients, associated with Z· decay, in a partially dehydrated wild-type sample at −10 °C (solid line), 4 °C (dotted line), and 21 °C (dashed line). As shown, the yield and decay of Z· were indistinguishable at these three different temperatures in wild-type PSII. However, this was not the case for partially dehydrated H190Q-D1 (Figure 4B), where a temperature dependence in the yield was observed. In this mutant, the yield of Z· was lower at higher temperatures. The yield at 4 °C (dotted line) was 70% of the −10 °C yield (solid line), and the yield at 21 °C (dashed line) was 40% of the −10 °C yield (solid line). However, there was no significant change in the overall kinetics of Z· decay at the three temperatures.

This observed temperature dependence in the H190Q-D1 mutant could be due either to a reversible or to an irreversible phenomenon. To distinguish between these two possibilities, measurements were performed on a H190Q-D1 sample at −10 °C (Figure 4C, solid line). The sample was warmed to 21 °C, and EPR transients were acquired (Figure 4C, dashed line). The sample was then cooled, and the −10 °C measurement was repeated (Figure 4C, dotted line). The resulting data show that the change in the yield of Z· is primarily reversible, because 80% of the single turnover yield was recovered when the sample was reequilibrated at −10 °C. Note that field-swept EPR spectra acquired under continuous illumination were indistinguishable at all three temperatures (data not shown).

In summary, in the H190Q-D1 and E189Q-D1 mutants, the yield of Z· is temperature-dependent, and the yield increases as the temperature decreases. The temperature effect is primarily reversible in the H190Q-D1 mutant. The effect of temperature can be explained by a conformational change that alters the oxidation rate either of tyrosine Z or of an alternate donor.

Difference FT-IR Measurements: 1800−1200 cm^{-1} Region. A Z· minus Z difference FT-IR spectrum will reflect those vibrational perturbations that occur upon tyrosine Z oxidation (*43*−*45*) and changes in the environment of tyrosine Z (*34*, *44*, *55*). Positive lines in the difference FT-IR spectrum arise from tyrosyl radical Z· and negative lines arise from tyrosine Z. The difference FT-IR spectrum acquired from wild-type PSII (Figure 5A) is similar to those from previous reports (*43*, *44*). To assign this spectrum, difference FT-IR spectra were obtained on tyrosyl radicals generated *in vitro* (*56*, *57*). Also, isotopomers of tyrosine have been incorporated into PSII. This approach identified the vibrational components that arise from Z· and Z in the Z· minus Z difference FT-IR spectrum (*43*, *44*, *58*). Finally, comparison of EPR and FT-IR-derived kinetics has also been used to assign vibrational bands (*45*). For example, using this approach, a positive line at 1478 cm^{-1} has been assigned to the CO vibration of Z·.

Figure 5 shows the 1800−1200 cm^{-1} region of Z· minus Z difference FT-IR spectra. These spectra were acquired under 4 min of continuous illumination on manganese-depleted wild-type (A), H190Q-D1 (B), and E189Q-D1 (C) PSII. The conditions were similar to those employed for EPR spectroscopy at −10 °C, and those experiments (Figure 2) show that the yield of Z· is similar in all three preparations. These FT-IR spectra are known to be dominated by donor side redox changes. For example, fluorescence experiments presented previously have shown that Q_A^- is not a significant contributor to the photo-steady state, under these conditions (*43*, *44*, *58*). This is important because the vibrations of Q_A and Q_A^- (*59*) overlap the Z· minus Z spectrum (*58*) and complicate data interpretation.

To identify the vibrational bands that are perturbed upon mutation of H190-D1 and E189-D1, we have constructed the double difference spectra (wild-type minus mutant) shown in panels E and F of Figure 5, respectively. In these double difference spectra, only those vibrations that are perturbed upon mutation will be observed. When His 190 of the D1 polypeptide was mutated to Gln, perturbations were observed in the 1800−1200 cm^{-1} region of the infrared spectrum (Figure 5E). The vibrational frequencies in the 1754−1700 cm^{-1} region are suggestive of the oxidation of chl *a* (*60*). One possibility is that these bands arise from increased PSI contamination in the H190Q-D1 mutant, as previously suggested (*20*). However, comparison of Figure 5E to the

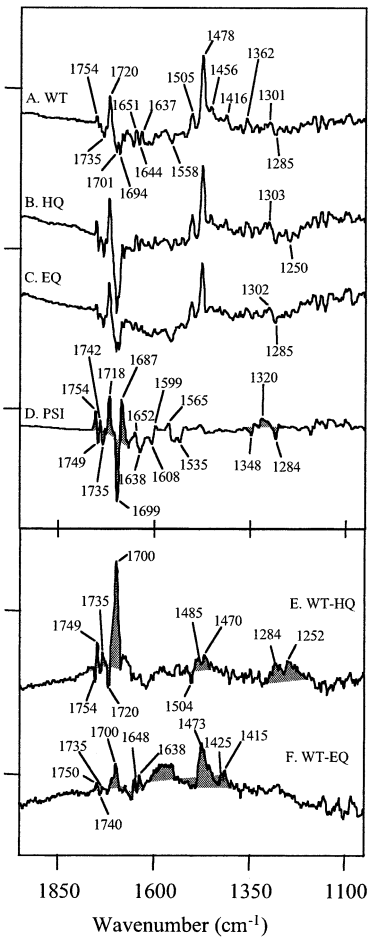

FIGURE 5: The 1800−1200 cm^{-1} region of the Z· minus Z difference FT-IR spectrum. Data were obtained on manganese-depleted PSII particles from wild-type (A), H190Q-D1 (B), and E189Q-D1 (C) under 4 min of continuous illumination. A P_{700}^{+} minus P_{700} difference FT-IR spectrum is shown in (D). Data were acquired on partially dehydrated samples at −10 °C. Samples were in 5 mM HEPES−NaOH, pH 7.5, and either 3 mM potassium ferricyanide and 3 mM potassium ferrocyanide (A−C) or 11 mM potassium ferricyanide and 11 mM potassium ferrocyanide (D). In the upper panel, tick marks on the *y*-axis are 4×10^{-4} AU. In the lower panel, the double difference spectra, (E) wild-type minus H190Q and (F) wild-type minus E189Q, are also shown. The tick marks on the *y*-axis in the lower panel are 2×10^{-4} AU. In each panel, the *y*-axis shows Δ absorbance.

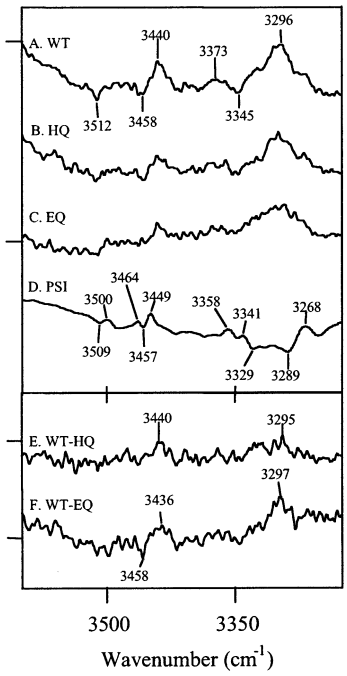

FIGURE 6: The 3600−3100 cm^{-1} region of the Z· minus Z difference FT-IR spectrum. Data were obtained on manganese-depleted PSII particles from wild-type (A), H190Q-D1 (B), and E189Q-D1 (C) under 4 min of continuous illumination. A P_{700}^{+} minus P_{700} difference FT-IR spectrum is shown in (D). Data were acquired on partially dehydrated samples at −10 °C. Samples were in 5 mM HEPES−NaOH, pH 7.5, and either 3 mM potassium ferricyanide and 3 mM potassium ferrocyanide (A−C) or 11 mM potassium ferricyanide and 11 mM potassium ferrocyanide (D). In the upper panel, tick marks on the *y*-axis are 3×10^{-4} AU. In the lower panel, the double difference spectra, (E) wild-type minus H190Q and (F) wild-type minus E189Q, are also shown. The tick marks on the *y*-axis in the lower panel are 1×10^{-4} AU. In each panel, the *y*-axis shows Δ absorbance.

light minus dark spectrum acquired from cyanobacterial PSI (see refs *39* and *46* and Figure 5D) shows that the two spectra are not identical. This is particularly evident in the 1350−1250 cm^{-1} region, which is expected to contain CO vibrations of chl. The PSI difference spectrum is also distinct in the OH/NH stretching region (see Figure 6). This comparison suggests that a chl molecule within PSII, such as Chl_Z (for example, see ref *61*), is oxidized in higher yield in the H190Q-D1, when compared to wild-type (see below). The observation of a broad positive band in the 1485−1470 cm^{-1} region is consistent with a Chl_Z^{+} assignment (*61*, *62*). An increased contribution from Chl_Z^{+} could arise from a structural alteration in the H190Q-D1 mutant. Note that the data do not resemble the spectrum associated with protonation of the imidazole side chain (*63*).

When Glu 189 of the D1 polypeptide is mutated to Gln, the double difference spectrum, wild-type minus E189Q (Figure 5F), is distinct from the H190Q double difference spectrum (Figure 5E) in most spectral regions. The 1750−1700 cm^{-1} region exhibits bands in common with the H190Q-D1 spectrum. This spectral similarity suggests that there is a small increased contribution of oxidized chl to this spectrum, as well as to the H190Q spectrum. However, the negative band at 1754 cm^{-1}, observed in Figure 5E, is not observed in Figure 5F. This result suggests a structural change involving the chl ester group in this mutant (*46*, *60*). Alternatively, these bands may arise from the C═O stretching vibrations of Asp and Glu residues. Positive bands between 1473 and 1415 cm^{-1} are consistent with an increased contribution to the wild-type spectrum from carboxylate residues (for a review of carboxylate vibrational modes, see ref *64* and references therein). Bands at 1648, 1638, and ∼1580 cm^{-1} are also observed. Overall, the spectrum does not resemble a glutamate protonation spectrum (*64*, *65*). These data are consistent with either a decreased spectral contribution from Glu 189 or another glutamate/aspartate in the E189Q-D1 FT-IR spectrum. This could occur because of a mutation-induced conformational change in the E189Q-D1 mutant.

Difference FT-IR Measurements: 3600−3100 cm^{-1} Region. Figure 6 shows the 3600−3100 cm^{-1} region of the difference FT-IR spectrum acquired from wild-type (A), H190Q-D1 (B), and E189Q-D1 (C). The spectrum in Figure 6A is similar to the D· minus D spectrum previously reported (*34*). Vibrational bands in this region were assigned to NH

stretching modes of the proton acceptor for tyrosine D and other amino acids in the environment of tyrosine D (*34*, *44*). The similarity of Figure 6A to the D· minus D spectrum (*34*, *44*) suggests a similar assignment for the Z· minus Z spectrum. Global ^{15}N-labeling experiments also support this conclusion (Kim and Barry, unpublished results). The PSI difference spectrum is distinct in this spectral region (Figure 6D). As shown in the double difference spectra, wild-type minus H190Q (Figure 6E) and wild-type minus E189Q (Figure 6F), the H190 mutation has little effect on these vibrational bands. However, the E189 mutation has a more significant effect, as evidenced by spectral contributions to the double difference spectrum at 3458, 3436, and 3297 cm^{-1} (Figure 6F). This result confirms that H190Q-D1 has only a minor effect on proton-transfer events involving tyrosine Z. The result also suggests that structural changes at E189Q are linked to tyrosine Z redox reactions.

DISCUSSION

Several studies report the effects of mutations at His 190 and Glu 189 on PSII function (*19*−*23*, *29*, *30*, *47*, *66*). E189Q-D1 has been reported to have an unaltered single turnover fluorescence yield and decay (*23*), an unaltered S_2 state multiline EPR signal (*24*), and unaltered electron-transfer rates from the manganese cluster/tyrosine Z to P_{680}^+ (*25*). However, the steady-state level of oxygen evolution activity is reduced by a factor of 2 in this mutant, and other mutations at E189 show more perturbed phenotypes (*23*).

The H190Q-D1 mutant is completely inactive in oxygen evolution (*20*, *23*). In some studies, H190 has been assigned as the immediate proton acceptor and proton donor for tyrosine Z (refs *21*−*23*, *30*, and *66* but see refs *19* and *20*). This conclusion was based on the apparent, dramatic effects of H190 mutations on all Z redox reactions at room temperature (*21*, *22*, *30*). Chemical complementation has shown that high concentrations of exogenous bases can partially restore electron-transfer rates in these mutants (*22*, *30*). In this report, we have applied fluorescence, EPR, and FT-IR spectroscopy and obtained new information concerning the role of His 190 and Glu 189 in PSII.

Fluorescence Results. In wild-type PSII, a rapid rise in fluorescence yield was observed, and the decay of fluorescence after the saturating flash had an overall half-time of 50 ms. This is similar to the rate constant for Z·Q_A^- recombination, which was determined from EPR measurements of Z· reduction kinetics (see below). This comparison suggests that the majority of Q_A^- is oxidized by recombination with Z· in wild-type cyanobacterial PSII, under these conditions. In manganese-depleted H190Q-D1 PSII, our results show a significant fluorescence yield after a saturating flash. This is a surprising result, given the conclusions in the literature, and is in contrast to our observations on intact H190Q-D1 cells. The fast component to the fluorescence yield is attributed to PSII centers in which Z reduces P_{680}^+, based on comparison with the EPR measurements of the Z· yield under similar conditions.

EPR Results. As assessed by EPR spectroscopy at room temperature, the single turnover yield of Z· was 38% of wild-type in H190Q-D1 PSII. However, at low temperature, the yield of Z· in H190Q-D1 increased by a factor of ∼2. An increase in Z· yield was also observed in the E189Q-D1 mutant. Experiments on the H190Q-D1 mutant showed that this increase in yield is reversible. Reversible temperature dependence suggests a reversible conformational change in the mutants. This conformational flexibility is induced by the mutations, because wild-type samples did not exhibit the same phenomena.

Rate of Z· Reduction. Under all conditions examined, EPR kinetic transients indicated that the overall half-times of Z· reduction in H190Q-D1, E189Q-D1, and wild-type were similar (190−280 ms). This result agrees with previous EPR studies of purified particles from *Chlamydomonas* H190F and H190Y (*19*). However, this result contradicts experiments conducted on *Chlamydomonas* membranes (*21*, *47*) and optical studies of purified PSII from cyanobacterial H190 mutants (*22*). The reasons for these discrepancies are not clear. In refs *21* and *47*, fluorescence experiments on *Chlamydomonas* H190F and H190Y mutants were conducted in thylakoid membranes. Perhaps a fluorescence quencher lowers signal amplitude in *Chlamydomonas* membranes, as a quencher apparently does in cyanobacterial cells (compare Figure 1A and Figure 1B). However, the explanation for the low EPR amplitudes observed in studies of those same *Chlamydomonas* membranes (*21*) remains to be determined. In ref *22*, in which cyanobacterial H190Q-D1 PSII particles were studied with optical spectroscopy, mutation-induced shifts in the UV spectrum of Z· may have occurred. Because Z· reduction kinetics were monitored at a single wavelength, such spectral shifts would complicate kinetic analysis.

Two parallel processes, recombination with Q_A^- and reduction by ferrocyanide, are expected to contribute to the overall rate of Z· reduction (*45*, *51*, *67*). On the basis of previous measurements (*45*, *51*, *67*), the 40 ms fast phase, observed here by EPR spectroscopy in wild-type, is assigned to recombination between Q_A^- and Z·. The 300 ms slow phase, observed here, is assigned to reduction of Z· by potassium ferrocyanide.

On the basis of this assignment of the fast and slow phases, we conclude that there is an slight increase in the rate of Z·Q_A^- recombination in the H190Q-D1 mutant and that this rate is unaffected in the E189Q-D1 mutant. There is no significant effect on the rate of Z· reduction by ferrocyanide in either mutant. Temperature appears to have no significant effect on either rate constant. Z· is known to be a neutral radical (*8*, *9*, *68*), and some studies have concluded that Z is protonated at pH 7.5 (*21*, *22*, *30*, *32*, *52*, *69*). If Z is protonated, then proton transfer must accompany the electron-transfer reactions. Our data suggest that His 190 and Glu 189 have no impact on proton and/or electron transfer to Z· under these conditions.

Rate of Z Oxidation. Because the rate of Z· reduction is relatively unaffected in H190Q-D1 and E189Q-D1, but the Z· yield is altered, we conclude that the main effect of the mutations is on the rate of Z oxidation by P_{680}^+ (see also refs *21*−*23*, *47*, and *66*). Previous studies have implicated a group with a pK_a of 5−8 as the proton acceptor for Z (*21*, *22*, *29*, *32*, *51*, *70*, *71*). It has been suggested that this group is His 190, with Glu 189 playing an auxiliary role in proton transfer. However, our results indicate that these roles for His 190 and Glu 189 are not likely. The effects of H190Q-D1 on the Z· yield are relatively modest. This is especially true at low temperature, where the H190Q-D1 yield differs from wild-type by less than a factor of 2. The effect of E189Q-D1 on the Z· yield is also relatively small. Because

the substituted glutamine side chains are not protonatable, these results argue against a role for either His 190 or Glu 189 as the sole or immediate proton acceptor for tyrosine Z. Instead, we propose that these residues modulate Z proton and/or electron-transfer reactions through a structural change in the PSII reaction center. An alternative explanation of our results is that the mutations alter a competing rate of electron transfer to P_{680}^+ and lead to an indirect effect on the yield of Z•.

Both fluorescence and EPR experiments demonstrate that the yield of Z• in H190Q-D1 centers, at room temperature, is 31−38% of wild-type. This is a surprising result in light of previous optical measurements on the H190Q-D1 mutant (*22*, *66*). In those experiments, the rate of P^+ reduction, as monitored at 432.5 or 810 nm, was observed to be slowed by 2−3 orders of magnitude in H190Q-D1, relative to wild-type. Our results suggest that such a dramatic decrease in rate cannot occur in all H190Q-D1 centers, because the rate of Z oxidation would not be significant relative to $P_{680}^+Q_A^-$ recombination reactions and Z• would not be observed (*72*). One way to reconcile our work with previous results is to propose that there is a distribution of the Z oxidation rate in the H190Q sample at room temperature. In this scenario, in 31−38% of H190Q-D1 centers, the rate of Z oxidation is similar to that of wild-type PSII. By similar, we mean significant with respect to the rate of the 0.8 ms $P_{680}^+Q_A^-$ back-reaction (*72*). In remaining centers, we postulate that the rate of Z oxidation has dramatically slowed and that those structurally destabilized centers do not significantly contribute to the yield of Z• in our experiments. Such a scenario might explain the results of refs *22* and *66*, if a small amplitude, fast kinetic phase was overlooked in that data analysis. Alternatively, the concentration of these putative, stable H190Q-D1 centers may be preparation-dependent, and these stable centers may have been absent or present at lower concentration in the PSII preparations employed in refs *22* and *66*. In the context of this scenario, we can explain the observed temperature effects in the H190Q-D1 mutant as a temperature-induced shift in the relative concentrations of stable and destabilized PSII centers.

Previous Chemical Complementation Data. Chemical complementation studies on His 190 mutants showed that the addition of exogenous bases could stimulate tyrosine Z redox reactions in wild-type and H190D1 mutants (*22*, *30*). That effect was interpreted to mean that His 190 acted as the immediate proton acceptor at room temperature. However, that work can be rationalized differently in the context of these results. In the studies of refs *22* and *30*, exogenous bases were added in high concentrations. These hydrogen-bonding compounds may provide structural stabilization or induce conformational changes at room temperature. These structural changes may accelerate the rate of Z oxidation in the H190Q-D1 mutant by shifting the equilibrium between stable and destabilized centers. Note that high concentrations of bases were also observed to have an effect on wild-type electron transfer (*22*). By contrast, chemical complementation studies on tyrosine D were performed at low concentration of imidazole, and significant effects on wild-type were not observed (*34*).

FT-IR Spectroscopy. Difference FT-IR spectroscopy was employed to study the role of His 190 and Glu 189. The Z• minus Z difference spectrum associated with H190Q-D1 has been reported at pH 6.0 (*20*). In the present work, at pH 7.5, an increased yield of Chl_Z^+ was observed in FT-IR spectra acquired from the H190Q-D1 mutant. This effect was observed when the samples were illuminated for 4 min or 1.3 s (data not shown). Chl perturbations were observed in previous FT-IR spectra acquired at pH 6.0 but were attributed to increased PSI contamination in the mutant (*20*). Our present data do not support that interpretation, because the PSI difference spectrum was observed to be distinct in the 1360−1200 and 3600−3100 cm^{-1} regions. Other changes in the spectrum were small but could be due to changes in protein conformation or the positions of amino acid side chains. We attribute these changes in the FT-IR spectrum to a structural change, which may shorten the distance between Chl_Z and P_{680}^+.

On the other hand, in the E189Q-D1 mutant, the FT-IR spectrum reveals mutation-induced perturbations to vibrational bands that are clearly assignable to glutamate and/or aspartate. This result suggests that E189 and tyrosine Z may be redox linked, perhaps via a long-distance change in structure or polarity.

Hydrogen Bonding. Magnetic resonance experiments suggest that Z• is involved in partially disordered hydrogen bonds (*26*−*29*, *73*). FT-IR studies, under the conditions used here, have not detected these hydrogen bonds (*20*, *44*). As shown in these experiments, wild-type, H190Q-D1, and E189Q-D1 have similar EPR Z• line shapes at both low and room temperature. These results are in agreement with data previously obtained (*19*, *20*). This spectral similarity suggests that an interaction, such as a hydrogen bond, between tyrosine Z and His 190 is not likely in manganese-depleted PSII. In contrast, when the hydrogen bond partner and proton donor/acceptor for tyrosine D, His189 D2, was mutated, dramatic effects on the D• EPR line shape were observed (*34*, *74*, *75*).

While hydrogen bonds to Z• have not been detected by FT-IR spectroscopy (*20*, *44*), this discrepancy could be explained if the hydrogen bond partners are water molecules. FT-IR samples are partially dehydrated (*44*). If Z• hydrogen bonds are to water, our work demonstrates that removal of water has no significant effect on the yield or EPR line shape of Z• (see also ref *44*).

Conclusion. The H190Q and E189Q mutations induce a reversible, temperature-dependent conformational change, which alters the redox properties of tyrosine Z. The H190Q-D1 mutation reduces the yield of Z• by a factor of 2.6 at room temperature but causes a less significant change at low temperature. There is no dramatic effect on the reduction of Z• in either mutant. Taken together, our data suggest that Glu 189 and His 190 provide structural stabilization on the donor side of PSII and that neither residue functions as the immediate proton acceptor for tyrosine Z.

ACKNOWLEDGMENT

The authors thank Dr. Bengt Svensson and Dr. Lorraine Anderson for helpful discussions. The authors are also grateful to Dr. Colette A. Sacksteder for providing the PSI difference FT-IR spectrum and to Prof. Neil Olszewski for use of equipment.

REFERENCES

1. Barry, B. A. (1995) *Methods Enzymol. 258*, 303−319.

2. Britt, R. D. (1996) in *Oxygenic Photosynthesis: The Light Reactions* (Yocum, C. F., Ed.) pp 137−164, Kluwer Academic Publishers, Dordrecht.
3. Shen, J.-R., and Kamiya, N. (2000) *Biochemistry 39*, 14739−14744.
4. Zouni, A., Witt, H. T., Kern, J., Fromme, P., Krauss, N., Saenger, W., and Orth, P. (2001) *Nature 409*, 739−743.
5. Debus, R. J., Barry, B. A., Sithole, I., Babcock, G. T., and McIntosh, L. (1988) *Biochemistry 27*, 9071−9074.
6. Metz, J. G., Nixon, P. J., Rögner, M., Brudvig, G. W., and Diner, B. A. (1989) *Biochemistry 28*, 6960−6969.
7. Noren, G. H., and Barry, B. A. (1992) *Biochemistry 31*, 3335−3342.
8. Boerner, R. J., and Barry, B. A. (1993) *J. Biol. Chem. 268*, 17151−17154.
9. Barry, B. A., and Babcock, G. T. (1987) *Proc. Natl. Acad. Sci. U.S.A. 84*, 7099−7103.
10. Debus, R. J., Barry, B. A., Babcock, G. T., and McIntosh, L. (1988) *Proc. Natl. Acad. Sci. U.S.A. 85*, 427−430.
11. Vermaas, W. F. J., Rutherford, A. W., and Hansson, Ö. (1988) *Proc. Natl. Acad. Sci. U.S.A. 85*, 8477−8481.
12. Trebst, A. (1986) *Z. Naturforsch. 41c*, 240−245.
13. Svensson, B., Vass, I., Cedergren, E., and Styring, S. (1990) *EMBO J. 7*, 2051−2059.
14. Ruffle, S. V., Donnelly, D., Blundell, T. L., and Nugent, J. H. A. (1992) *Photosynth. Res. 34*, 287−300.
15. Koulougliotis, D., Tang, X.-S., Diner, B. A., and Brudvig, G. W. (1995) *Biochemistry 34*, 2850−2856.
16. Boska, M., Sauer, K., Buttner, W., and Babcock, G. T. (1983) *Biochim. Biophys. Acta 722*, 327−330.
17. Boussac, A., and Etienne, A. L. (1984) *Biochim. Biophys. Acta 766*, 576−581.
18. Vass, I., and Styring, S. (1991) *Biochemistry 30*, 830−839.
19. Roffey, R. A., van Wijk, K. J., Sayre, R. T., and Styring, S. (1994) *J. Biol. Chem. 269*, 5115−5121.
20. Bernard, M. T., MacDonald, G. M., Nguyen, A. P., Debus, R. J., and Barry, B. A. (1995) *J. Biol. Chem. 270*, 1589−1594.
21. Mamedov, F., Sayre, R. T., and Styring, S. (1998) *Biochemistry 37*, 14245−14256.
22. Hays, A.-M. A., Vassiliev, I. R., Golbeck, J. H., and Debus, R. J. (1998) *Biochemistry 37*, 11352−11365.
23. Chu, H.-A., Nguyen, A. P., and Debus, R. J. (1995) *Biochemistry 34*, 5839−5858.
24. Debus, R. J., Campbell, K. A., Pham, D. P., Hays, A.-M. M., and Britt, R. D. (2000) *Biochemistry 39*, 6275−6287.
25. Clausen, J., Winkler, S., Hays, A.-M. A., Hundelt, M., Debus, R. J., and Junge, W. (2001) *Biochim. Biophys. Acta 1506*, 224−235.
26. Force, D. A., Randall, D. W., Britt, R. D., Tang, X.-S., and Diner, B. A. (1995) *J. Am. Chem. Soc. 117*, 12643−12644.
27. Un, S., Tang, X.-S., and Diner, B. A. (1996) *Biochemistry 35*, 679−684.
28. Tang, X. S., Zheng, M., Chisholm, D. A., Dismukes, G. C., and Diner, B. A. (1996) *Biochemistry 35*, 1475−1484.
29. Diner, B. A., Force, D. A., Randall, D. W., and Britt, R. D. (1998) *Biochemistry 37*, 17931−17943.
30. Hays, A.-M. A., Vassiliev, I. R., Golbeck, J. H., and Debus, R. J. (1999) *Biochemistry 38*, 11851−11865.
31. Haumann, M., Bogershausen, O., Cherepanov, D., Ahlbrink, R., and Junge, W. (1997) *Photosynth. Res. 51*, 193−208.
32. Rappaport, F., and Lavergne, J. (1997) *Biochemistry 36*, 15294−15302.
33. Lydakis-Simantiris, N., Ghanotakis, D. F., and Babcock, G. T. (1997) *Biochim. Biophys. Acta 1322*, 129−140.
34. Kim, S., Liang, J., and Barry, B. A. (1997) *Proc. Natl. Acad. Sci. U.S.A. 94*, 14406−14412.
35. Zouni, A., Kern, J., Loll, B., Fromme, P., Orth, P., Krauss, N., Saenger, W., and Biesiadka, J. (2002) in *Proceedings of the 12th International Congress on Photosynthesis* (Voesenek, R., Ed.) pp S05−003, Thieme, Stuttgart.
36. Rippka, R., Derulles, J., Waterbury, J. B., Herdman, M., and Stanier, R. (1979) *J. Gen. Microbiol. 111*, 1−61.
37. Williams, J. G. K. (1988) *Methods Enyzmol. 167*, 766−778.
38. Noren, G. H., Boerner, R. J., and Barry, B. A. (1991) *Biochemistry 30*, 3943−3950.
39. Kim, S., Sacksteder, C. A., Bixby, K. A., and Barry, B. A. (2001) *Biochemistry 40*, 15384−15395.
40. Lichtenthaler, H. K. (1987) *Methods Enzymol. 148*, 350−382.
41. Steenhuis, J. J., and Barry, B. A. (1998) *J. Phys. Chem. B 102*, 4−8.
42. Boerner, R. J., Nguyen, A. P., Barry, B. A., and Debus, R. J. (1992) *Biochemistry 31*, 6660−6672.
43. Kim, S., Ayala, I., Steenhuis, J. J., Gonzalez, E. T., Razeghifard, M. R., and Barry, B. A. (1998) *Biochim. Biophys. Acta 1364*, 337−360.
44. Kim, S., and Barry, B. A. (1998) *Biophys. J. 74*, 2588−2600.
45. Ayala, I., Kim, S., and Barry, B. A. (1999) *Biophys. J. 77*, 2137−2144.
46. Kim, S., and Barry, B. A. (2000) *J. Am. Chem. Soc. 122*, 4980−4981.
47. Roffey, R. A., Kramer, D. A., Govindjee, and Sayre, R. T. (1994) *Biochim. Biophys. Acta 1184*, 257−270.
48. Blankenship, R. E., Babcock, G. T., Warden, J. T., and Sauer, K. (1975) *FEBS Lett. 51*, 287−293.
49. Warden, J. T., Blankenship, R. E., and Sauer, K. (1976) *Biochim. Biophys. Acta 423*, 462−478.
50. Reinman, S., and Mathis, P. (1981) *Biochim. Biophys. Acta 635*, 249−258.
51. Shigemori, K., Miro, H., and Kawamori, A. (1997) *Plant Cell Physiol. 38*, 1007−1011.
52. Kühne, H., and Brudvig, G. W. (2002) *J. Phys. Chem. B* (in press).
53. Miller, A.-F., and Brudvig, G. W. (1991) *Biochim. Biophys. Acta 1056*, 1−18.
54. Ma, C., and Barry, B. A. (1996) *Biophys. J. 71*, 1961−1972.
55. Kim, S., and Barry, B. A. (2001) *J. Phys. Chem. B 105*, 4072−4083.
56. Cappuccio, J. A., Ayala, I., Elliot, G. I., Szundi, I., Lewis, J., Konopelski, J. P., Barry, B. A., and Einarsdottir, O. (2002) *J. Am. Chem. Soc. 124*, 1750−1760.
57. Ayala, I., Range, K., York, D., and Barry, B. A. (2002) *J. Am. Chem. Soc. 124*, 5496−5505.
58. Kim, S., Patzlaff, J. S., Krick, T., Ayala, I., Sachs, R. K., and Barry, B. A. (2000) *J. Phys. Chem. B 104*, 9720−9727.
59. Razeghifard, M. R., Kim, S., Patzlaff, J. S., Hutchison, R. S., Krick, T., Ayala, I., Steenhuis, J. J., Boesch, S. E., Wheeler, R. A., and Barry, B. A. (1999) *J. Phys. Chem. B 103*, 9790−9800.
60. Nabedryk, E., Leonhard, M., Mantele, W., and Breton, J. (1990) *Biochemistry 29*, 3242−3247.
61. Tracewell, C. A., Cua, A., Stewart, D. H., Bocian, D. F., and Brudvig, G. W. (2001) *Biochemistry 40*, 193−203.
62. MacDonald, G. M., Steenhuis, J. J., and Barry, B. A. (1995) *J. Biol. Chem. 270*, 8420−8428.
63. MacDonald, G. M., and Barry, B. A. (1992) *Biochemistry 31*, 9848−9856.
64. Hutchison, R. S., Steenhuis, J. J., Yocum, C. F., Razeghifard, M. R., and Barry, B. A. (1999) *J. Biol. Chem. 274*, 31987−31995.
65. Steenhuis, J. J., and Barry, B. A. (1997) *J. Phys. Chem. B 101*, 6652−6660.
66. Diner, B. A., Nixon, P. J., and Farchaus, J. W. (1991) *Curr. Opin. Struct. Biol. 1*, 546−554.
67. Dekker, J. P., van Gorkom, H. J., Brok, M., and Ouwehand, L. (1984) *Biochim. Biophys. Acta 764*, 301−309.
68. Barry, B. A., El-Deeb, M. K., Sandusky, P. O., and Babcock, G. T. (1990) *J. Biol. Chem. 265*, 20139−20143.
69. Haumann, M., Mulkidjanian, A., and Junge, W. (1999) *Biochemistry 38*, 1258−1267.
70. Conjeaud, H., and Mathis, P. (1980) *Biochim. Biophys. Acta 590*, 353−359.
71. Ahlbrink, R., Haumann, M., Cherepanov, D., Bogershausen, O., Mulkidjanian, A., and Junge, W. (1998) *Biochemistry 37*, 1131−1142.
72. Buser, C. A., Thompson, L. K., Diner, B. A., and Brudvig, G. W. (1990) *Biochemistry 29*, 8977−8985.
73. Mino, H., Astashkin, A. V., and Kawamori, A. (1997) *Spectrochim. Acta, Part A 53*, 1465−1483.
74. Tommos, C., Davidsson, L., Svensson, B., Madsen, C., Vermaas, W., and Styring, S. (1993) *Biochemistry 32*, 5436−5441.
75. Tang, X.-S., Chisholm, D. A., Dismukes, G. C., Brudvig, G. W., and Diner, B. A. (1993) *Biochemistry 32*, 13742−13748.

BI026172L